

Supporting Information

Kitamura et al. 10.1073/pnas.1002372107

SI Methods

Mouse Strains. C57BL/6 and *nu/nu* BALB/c mice were purchased from CLEA Japan. *Ccr1*^{-/-} mice and *Mmp7*^{-/-} mice were obtained from Taconic and Jackson Laboratory, respectively. EGFP transgenic mice, *Mmp2*^{-/-} mice, and *Mmp9*^{-/-} mice were provided by Drs. Okabe (Osaka University, Suita, Japan), Ito-hara (RIKEN Brain Science Institute, Wako, Japan), and Werb (University of California, San Francisco, CA), respectively. The *Mmp9*^{+/-} mice were derived from 129/Sv embryonic stem cells and backcrossed to C57BL/6 mice to the N₃ generation. Female *Mmp9*^{-/-} mice produced from N₃ interbreeding were used as hosts of tumor injections. *Ccr1*^{-/-}, *Mmp2*^{-/-}, *Mmp7*^{-/-}, and EGFP-transgenic mice were backcrossed to a C57BL/6 strain for more than 10 generations.

Experimental Metastasis Models. The experiments in Fig. 3B and C were conducted using different hosts. In Fig. 3B, nude mice were used as hosts, because they were more suitable for repeated live imaging (lack of hair helps obtain accurate photon counting). In Fig. 3C, we used syngeneic C57BL/6 mice as hosts because images were taken only twice on days 1 and 14 (when abdominal hair was removed before imaging).

Construction of Luciferase-Expressing Cells. CMT93, HT29, and HCT116 cells were transfected with pEF6 vector (Invitrogen) containing a firefly-luciferase gene by Lipofectamine 2000 (Invitrogen). We selected the clones that were resistant to blasticidin (Invitrogen) and determined their luciferase activities using Multilabel Reader Mithras (Berthold). Some of the luciferase-expressing clones were further transfected with *CCL15* gene, or shRNA against *Ccl9* or *CCL15* using lentiviral vectors (see below).

Lentiviral Expression Vector. The cDNA for active *CCL15*, which lacked 24 amino acids near NH₂ terminus (residues no. 22–45), was amplified by PCR using following primers; *NheI*-hCCL15Δ24-Fw: GCTAGCAGGAGGATGAAGGTCTCCGTGGCTGCCCTC-TCCCTGCCTCATGCTTGTGCTGTC CTGGATCCCAGGC-CAGCTTTCACCTTTGCTGCTGA, and hCCL15Δ24-Rv-XhoI: CTCGAGTTATAT TGATAGGGCTTCAGC. The amplified cDNA was cloned into the *NheI/XhoI* sites of pLEX-MCS vector (Open Biosystems).

Lentiviral shRNA Vector. The following sets of oligonucleotides were used to knockdown *CCL9* or *CCL15* expression; sh*Ccl9*#1-sense: CCGAAGTCCAGAGCAGTCTGAAGGCTCGAGC-CTTCAGACTGCTCGACTTTTTTTG
and sh*Ccl9*#1-antisense: AATTCAAAAAAAGTCCA-GAGCAGTCTGAAGGCTCGAGCCTTCAGACTGCTCTG-GACTT, sh*Ccl9*#2-sense: CCGGAACCACGGACCTACAAA-CAATCTCGAGATTGTTTGTAGGTCCGTGGTTTTTTT
and sh*Ccl9*#2-antisense: AATTCAAAAAAACCACGGAC-CTACAAAATCTCGAGATTGTTTGTAGGTCCGTG-GTT, sh*CCL15*#1-sense: CCGGGATGCAGAGACAGAG-TTAATGCTCGAGCATTAACTCTGTCTCTGCATCTTTT-TG
and sh*CCL15*#1-antisense: AATTCAAAAAGATGCAGA-GACAGAGTTAATGCTCGAGCATTAACTCTGTCTCTG-CATC,
and sh*CCL15*#2-sense: CCGGAATCCAGTAGTTCTGAA-CAGCCTCGAGGCTGTTCCAGAACTACTGGATTTTTTTG

and sh*CCL15*#2-antisense: CCGGAATCCAGTAGTTCT-GAACAGCCTCGAGGCTGTTCCAGAACTACTGGATTTTT-TTG.

Each set of oligonucleotides were annealed and cloned into the *AgeI/EcoRI* sites of pLKO.1 (Addgene).

Production and Infection of Lentiviruses. HEK293T cells were cotransfected with psPAX2 (Addgene), pMD2.G (Addgene), and pLKO.1 or pLEX-MCS by Lipofectamine 2000 (Invitrogen). After 48 h, cultured media were harvested and filtered through a sterile 0.45-μm filter (Millipore). The media containing lentiviral particles were added into the luciferase-expressing tumor cells (described above) with 8 μg/mL of polybrene (Millipore). Virus infected cells were selected by puromycin or hygromycin.

RT-PCR. The following sets of primers were used to determine mRNA levels;

Ccr1 (F: 5'-GCCCTGAGGGCCCCGAAGTGTACT -3', R: 5'-CAGACGCACGGCTTTGACCTTCTT -3'),
Cd34 (F: 5'-GCTCT GGAATCCGAGAAGTG-3', R: 5'-CCC-AAAGGTCAGAGATTGGA-3'), *Cd31/Pecam1* (F: 5'-AT-GACC CAGCAACATTCACA-3', R: 5'-GTCTCTGTGGC-TCTCGTTCC-3'), *Ccl3* (F: 5'-GGTCTCCACACTGC CCTT-3', R: 5'-TCAGGCATTTCAGTTCCAGGTC-3'),
Ccl4 (F: 5'-GAAGCTCTGCGTGTCTGCCCT-3', R: 5'-ACT-CCAAGTCACTCATGTACT-3'),
Ccl5 (F: 5'-ATGAAGATCTCTGCAGCTGCC-3', R: 5'-CTA-GTTCATCTCCAAATAGTT-3'),
Ccl6 (F: 5'-AGGATGAGAACTCCAAGACTG-3', R: 5'-TCAAGCAAT GACCTTGTTCCTCA-3'),
Ccl7 (F: 5'-AGCTACAGAAGGATCACCAG-3', R: 5'-CA-ATTCTACAGAC AGCTC-3'),
Ccl9 (F: 5'-ATGAAGCCTTTTTCATACTGCCCTC-3', R: 5'-TTATTGTTTGTAGGTCCGTG GTTG-3'), *Mmp2* (F: 5'-GCAAGTTCCCGTTCCTCC-3', R: 5'-CAGTACCAGT-GTCAGTATCAGC -3'), *Mmp7* (F: 5'-GCGGAGATGCT-CACTTTGAC-3', R: 5'-GCATCTATCACAGCGTGTTC-3'),
Mmp9 (F: 5'-TACAGGGCCCTTCCTTACT-3', R: 5'-ACTC-CTTATCCACGCGAATG-3'),
Mmp13 (F: 5'- AAT TCTGGGCTCTGAATGGTTA -3', R: 5'-GAATTTGTTGGCATGACTCTCA-3'), *Mmp14* (F: 5'-GCTCC GAGGAGAGATGTTT-3', R: 5'-CATCACTG-CCCATG AATGAC-3'),
Adam19 (F: 5'-ATGGCCAATA CAGGAAGTGC-3', R: 5'-CAGAAGTCCCAACACGAAGA-3'), *Adams15* (F: 5'-CAA-GTAGAGCAGC CAGATAACAGA-3', R: 5'-GGTCTCAAGACGAGAAGTCTAAT-3'),
Ctse (F: 5'-ATGCAGAGTTTGA TGGGATTCT-3', R: 5'-GCC-TCTTGAAGCTGTTTGTATCT-3'),
Ctsf (F: 5'-TTGGATTGTGACAAGGTG GA-3', R: 5'-CTT-GATGGCCAGTAAGGAA-3'),
Gapdh (F: 5'-CCTTCATTGACCTCAACTAC-3', R: 5'-TGG-GCCCTCAGATGCCTGCT-3'),
CCL3 (F: 5'-GCTAGCATCATGCAGGTCTCCACTGCTG-3', R: 5'-CTCGAGTCAGGCACTCAGCTCCAGGTCG-3'),
CCL4 (F: 5'-GCTAGCACCATGAAGCTCTGC GTGACTG-3', R: 5'-CTCGAGTCAGTTTCAGTTCCAGGTCATAC-3'),
CCL5 (F: 5'-GCTAGCACCATG AAGGTCTCCGCGGCAG-3',

R: 5'-CTCGAGCTAGCTCATCTCCAAAGAGTTG-3'),
CCL7 (F: 5'-GCTAGCAACATGAAAGCCTCTGCAGCAC-3',
 R: 5'-CTCGAGTCAAAGCTTTGGAGTTTGGGTT-3'),
CCL14 (F: 5'-GCTAGCAGCATGAAGATCTCCGTGG-
 CTG-3',
 R: 5'-CTCGAGTCAGTTCTCCTTCATGTCCTTG-3'),
CCL15 (F: 5'-GCTAGCAGGAGGATGAAGGTCTCCG-
 TGG-3',
 R: 5'-CTCGAGTTATATTGAGTAGGGCTTCAGC-3'),
CCL16 (F: 5'-GCTAGCAGGATGAAGGTCTCCGAGG-
 CTG-3',
 R: 5'-CTCGAGTCACTGGGAGTTGAGGAGCTGG-3'),
CCL23 (F: 5'-GCTAGCAGGAGGATGAAGGTCTC
 TGG-3',
 R: 5'-CTCGAGTCAATTCTTCCTGGTCTTGATC-3'), and
GAPDH (F: 5'-AGCTCCCGGA AAAGATTGAT-3', R: 5'-
 TTGGTTCTCCAGCTTCAGGT-3').

Histological Analyses. Mouse and human tissues were fixed with 4% paraformaldehyde and 10% formaldehyde, respectively. Tissues were embedded in paraffin wax, sectioned at 4- μ m thickness, and stained with H&E or processed for further staining. For immunostaining, the following antibodies were used as primary antibodies: rabbit polyclonal antibodies for GFP (Molecular Probes) and MMP7 (Calbiochem), a goat polyclonal antibody for MIP-1 γ /CCL9 (R&D Systems), a mouse monoclonal antibody for MMP13 (AnaSpec), and a guinea pig polyclonal antibody for CCL15 that we raised (see below). Staining signals were detected using Vectorstatin Elite ABC Kit (Vector Laboratories) and Peroxidase Substrate Kit DAB (Vector Laboratories). For immunofluorescence staining, tissues were directly embedded in O.C.T. Compound (Sakura Finetek), and sectioned at 6 μ m thickness. The sections were fixed with ice-cold acetone and immunostained using the following primary antibodies: a mouse monoclonal antibody for α SMA (DAKO Cytomation); rat monoclonal antibodies for F4/80 (Serotec), CD31, CD34, CD45 (BD Biosciences), CD11b, Gr-1, B2.20 (eBioscience), and CD14 (BioLegend); a hamster monoclonal antibody for CD11c (BD Biosciences); a chicken polyclonal antibody for CD3 ϵ (Santa Cruz Biotechnology), and rabbit polyclonal antibodies for pan-cytokeratin (DAKO), CCR1 (Santa Cruz Biotechnology), MMP2 (Lab Vision), and MMP9 (Abcam). Antibodies for IgG labeled with Alexa Fluor 488, Alexa Fluor 594 (Molecular Probes), or FITC (Jackson Immuno Research Laboratories) were used as secondary antibodies. Nuclei were stained with DAPI (Molecular Probes). Brightfield and fluorescence images were captured with Nikon ECLIPSE E800 and Leica CTR6000 fluorescent microscope, respectively. The captured images were analyzed with Adobe Photoshop software.

Development of Polyclonal Antibody for CCL15. The cDNA for CCL15 lacking signal peptide (1–21 aa) was amplified by PCR, and cloned into the pET15b vector (Novagen) that allowed incorporation of a histidine (6xHis) tag into the N terminus of CCL15. The expression plasmid was introduced into BL21 bacterial cells, and induced by 4-h incubation of the cells at 28 °C with 1 mM IPTG. The induced BL21 cells were sonicated in binding buffer (Novagen) and centrifuged to collect inclusion bodies. The inclusion bodies were solubilized by Binding buffer with 8 M urea and applied to a column containing Ni-NTA His Bind Resin (Novagen). For refolding of the His-CCL15 protein, the column was washed by wash buffer (Novagen) with urea at successive concentrations of 6, 4, 3, 2, 1, and 0 M. The refolded protein was eluted by Elute buffer (Novagen), and concentrated using Amicon Ultra15 (Millipore). The purified His-CCL15 protein was mixed with an adjuvant and injected into guinea pigs five times (TaKaRa). Whole antisera were collected from immunized animals, and polyclonal IgG was purified using Protein-G Sepharose (GE Healthcare).

Bone Marrow Transplantation. We injected 1×10^6 of bone-marrow cells isolated from EGFP transgenic mice into the tail vein of 4-wk-old recipient C57/BL6 mice that we had irradiated with 8-Gy γ -ray. Four weeks after bone marrow transplantation, the recipients were received intrasplenic tumor injection as described in *Methods*.

Proliferation in Culture. Tumor cell proliferation rate in culture was quantified using Cell Titer 96 Aqueous One Solution Cell Proliferation Assay (Promega) according to the manufacturer's protocol.

DNA Microarray. Liver metastasis foci were dissected from the wild-type and *Ccr1*^{-/-} mice using laser microdissection, and total RNAs were purified with RNeasy Micro Kit (Qiagen). Outside services from TORAY were used for the following experiments: verification of RNA quality by Agilent Bioanalyzer 2100 (Agilent Technologies), synthesis and Cy-dye labeling of aminoallyl RNA by Amino Allyl MessengerAmp II aRNA amplification Kit (Ambion), and hybridization to 3D-Gene DNA chips (TORAY).

CCR1 Inhibitor BL5923. The BL5923 is highly specific inhibitor to CCR1, and no other chemokine receptors are inhibited to any significant extents at the dosage used. Namely, we have tested a panel of additional chemokine receptors including human CCR2, CCR4, CCR5, CCR6, CCR7, CXCR1, CXCR2, and CXCR3 and in all cases the IC₅₀ in the binding assay was >10 μ M. The compound is also highly potent for human and mouse CCR1 with IC₅₀ of 20.4 ± 13.6 nM and 22.8 ± 11.1 nM, respectively, in the binding assay. Therefore, BL5923 has a similar potency for the human and mouse receptor. Due to the short half-life of BL5923 ($t_{1/2} = 3$ h), the high dose used here is required to obtain constant and full CCR1 blockade.

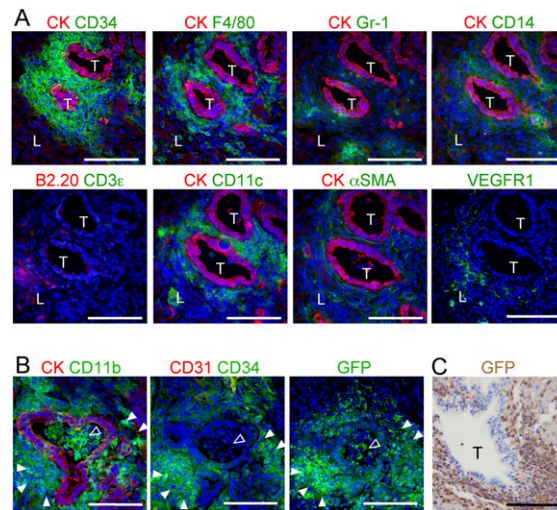


Fig. S1. Characterization of stromal cells surrounding disseminated cancer cells in the liver. (A) Serial sections were immunostained for the following markers; pan-cytokeratin (CK; a marker for epithelial cells), CD34 (myeloid progenitors), F4/80 (macrophages), Gr-1 (granulocytes), CD14 (monocytes), B2.20 (B cells), CD3 ϵ (T cells), CD11c (dendritic cells), α SMA (myofibroblasts), and VEGFR1 (endothelial cells). T, metastasizing tumor; L, adjacent normal liver. (Scale bars, 100 μ m.) (B and C) Liver metastasis foci in mice transplanted with GFP $^{+}$ bone-marrow cells. (B) Adjoining sections show immunostaining for the indicated cell markers or autofluorescence of GFP. (C) A paraffin section immunostained for GFP (hematoxylin counterstaining). Open arrowheads, leukocytes; filled arrowheads, clusters of the iMCs. T, tumor. (Scale bars, 100 μ m.)

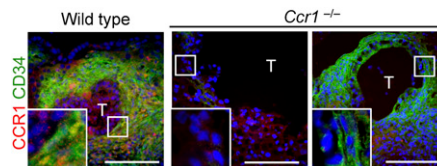


Fig. S2. Accumulation of the CD34 $^{+}$ iMCs in the liver foci of *Ccr1* $^{-/-}$ mice. Liver metastasis foci in wild-type and *Ccr1* $^{-/-}$ mice were stained for CD34 and CCR1. (Insets) Higher magnifications of the boxed areas. In the *Ccr1* $^{-/-}$ mice, most foci consisted of cystic tumor glands without accompanying iMCs (Center). As an exception, there were rare small foci with iMC accumulation (Right). T, tumor. (Scale bars, 100 μ m.)

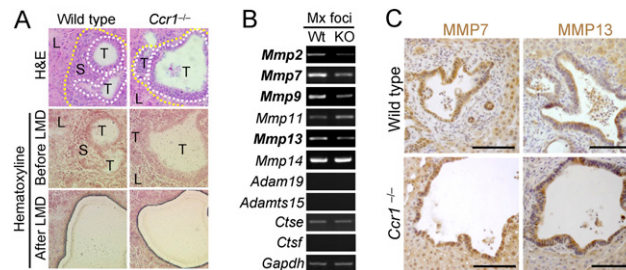


Fig. S3. Expression of various proteases in the metastatic foci of wild-type and *Ccr1* $^{-/-}$ mice injected with CMT93 cells. (A) Liver metastasis lesions stained with H&E (Top) or hematoxyline alone (Middle and Bottom). Metastatic foci including tumor cells (T) and stromal cells (S) were dissected by laser microdissection (LMD) from mice of each group (before and after LMD; Middle and Bottom, respectively). L, adjacent normal liver. (B) Expression of protease mRNAs analyzed by RT-PCR. Total RNA was isolated from the metastatic foci (Mx foci) in wild-type (Wt) and *Ccr1* $^{-/-}$ (KO) mice where the iMCs were associated or not, respectively. Of note, levels of *Mmp11*, *Adam19*, *Adamts15*, *Ctse*, and *Ctsf* were twofold higher in wild-type liver foci than *Ccr1* $^{-/-}$ in microarray data, although these results were not confirmed by RT-PCR. (C) Metastatic foci in the liver of wild-type and *Ccr1* $^{-/-}$ mice immunostained for MMP7 and MMP13 (hematoxylin counterstaining). (Scale bars, 100 μ m.)

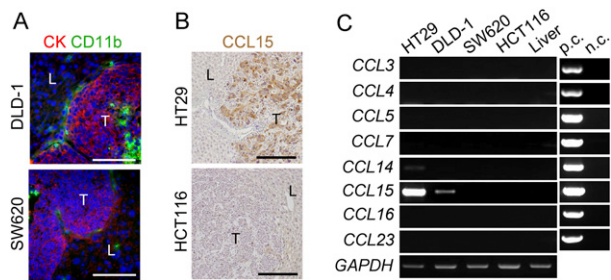


Fig. 54. Expression of CCR1 ligands in various human colon cancer cell lines. (A) Liver metastasis foci formed by DLD-1 or SW620 cells. T; tumor; L; liver. (Scale bars, 100 μ m.) (B) Liver metastasis foci in mice injected with HT29 or HCT116 cells. Paraffin sections were immunostained for CCL15 (hematoxylin counterstaining). T, tumor; L, adjacent normal liver. (Scale bars, 100 μ m.) (C) Expression of mRNAs for human CCR1 ligands determined by RT-PCR. Total RNA was isolated from human colon cancer cells HT29, DLD-1, SW620 and HCT116, and normal mouse liver (Liver). Commercially available cDNA clones were used as positive controls (p.c.). Negative controls (n.c.) had distilled water instead of RNA.

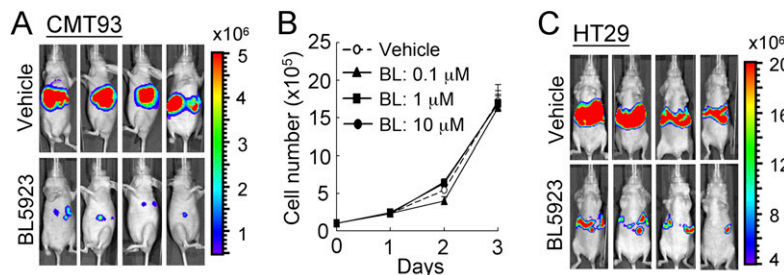


Fig. 55. Suppressive effects of CCR1 antagonist BL5923. (A) *In vivo* bioluminescence images of representative CMT93-injected mice treated with vehicle (Upper) or BL5923 at 50 mg/kg (Lower). Panels show four typical mice in each group analyzed at day 14 postinjection. (B) Proliferation of CMT93 cells cultured in the absence (Vehicle) or presence of BL5923 at 0.1, 1, and 10 μ M. Results are given as the means \pm SD ($n = 3$ experiments) (C) *In vivo* bioluminescence images of representative HT29-injected mice treated with vehicle (top) or BL5923 at 50 mg/kg (bottom). Panels show four typical mice in each group analyzed at day 28 postinjection.

Table S1. Mutations in human colon cancer cell lines used

Cell line	CCL15*	Wnt	TGFb	KRAS	PIK3CA	p53	BRAF	Other
HT29 (WiDr)	+++	APC	SMAD4	–	P449T [¶]	R273H	V600E	
LS174T	++	CTNNB1	T β R2	G12D	H1047R	–	–	UTX
LoVo	+	APC	–	G13D	–	–	–	FBXW7
Colo205	++	APC	SMAD4 [†]	–	–	Mut [†]	V600E	
T84	+++	APC	–	G13D	E542K	Mut [†]	–	
CaCo2	++	APC	SMAD4 [†]	–	No Data	Mut	No Data	No Data
HCT116	–	CTNNB1	T β R2	G13D	H1047R	–	–	CDKN2A MLH1
SW620 (SW480)	–	APC	SMAD4 [†]	G12V	–	R273H	–	
RKO	–	–	T β R2	–	H1047R	–	V600E	NF1
HCA7	–	–	T β R2	No Data	No Data	Mut	No Data	No Data
HCT15 (DLD1)	–	APC	T β R2	G13D	E545K	S241F	–	BRCA2 FAM123B MSH6

Signaling pathways in mouse colon cancer cell line CMT93^{††}

	Ccl9*	Wnt	TGFb	KRAS	PIK3CA	p53	BRAF	Other
CMT93	+++	Intact [†]	Intact [†]	No mutation [‡]	PI3K/Aktactivated [§]		No mutation ^{**}	STAT3 activated ^{††}

Mutational information on the human colon cancer cell lines were obtained from the COSMIC Library (Catalogue of Somatic Mutations in Cancer) provided by the Sanger Institute (<http://www.sanger.ac.uk/genetics/CGP/cosmic/>) and some papers.

*Levels of expression estimated by RT-PCR and ELISA.

[†]Evaluated by luciferase-reporters.

[‡]Sequencing of hot spots at codons 12, 13 and 61.

[§]Determined by phosphorylation of signaling proteins upon starvation.

[¶]Some mutations are found but causal relationship with cancer remains unknown.

^{||}No nuclear over-expression by immunohistochemistry; does not appear to be mutated.

^{**}No mutation in mouse BRAF at V637 (equivalent to human BRAF V600).

^{††}This cell line was of Subtype I as reported by Inai et al. (1).

1. Inai, et al. (2008) Comparative characterization of mouse rectum CMT93-I and -II cells by expression of claudin isoforms and tight junction morphology and function. *Histochem Cell Biol* 129:223.